*Int. J. Electrochem. Sci.*, 11 **(2016)** 200 - 214

**International Journal of ELECTROCHEMICAL SCIENCE**
www.electrochemsci.org

# N, P and Si tri-doped C Synthesized from Thiamine for $O_2$ Reduction Reaction under Alkaline Conditions

*Sunil Kumar Ramasahayam*[*], *Tito Viswanathan*[*]

Department of Chemistry, University of Arkansas at Little Rock, 2801 S. University Ave, Little Rock, AR 72204, USA
[*]E-mail: sxramasahaya@ualr.edu, txviswanatha@ualr.edu

*Received:* 22 October 2015 / *Accepted:* 11 November 2015 / *Published:* 1 December 2015

---

$O_2$ reduction reaction (ORR) at cathode plays an important role in the overall efficiency of a fuel cell. Renewable resource (thiamine) based electrocatalysts have been developed using a simple, rapid and inexpensive microwave assisted method without employing any reducing gases. Thiamine was used as the source of N, Silicone fluid as the source of Si and ammonium polyphosphate as the dehydrating agent and P, N source. Three kinds of N, P and Si doped C (NPSiDC) electrocatalysts, namely NPSiDC-1, NPSiDC-2 and NPSiDC-3 were prepared. NPSiDCs showed promise in ORR under alkaline conditions with peak potentials ranging from 0.542 V to 0.575 V vs. RHE (Reversible Hydrogen Electrode). From Koutecky-Levich studies, the mechanism of ORR was discovered to be a 4 $e^-$ process. Also, electrochemical stability studies revealed NPSiDC-2 to be stable over 2000 cycles in 0.1M KOH.

---

**Keywords:** electrocatalyst; fuel cell; microwave; $O_2$ reduction reaction; renewable resource.

## 1. INTRODUCTION

The hydrogen oxidation reaction at anode in a fuel cell has a lower oxidation overpotential and hence higher kinetic rate [1]. But, the oxygen reduction reaction (ORR) at cathode has a higher reduction overpotential due to low reaction rate [1]. Therefore, the efficiency of the fuel cell is dictated by this major limiting factor viz. oxygen reduction reaction at the cathode [2,3]. Traditionally, Pt-based catalysts were widely used in fuel cells to promote ORR [4-6]. However, they suffer from low kinetic rate, time and voltage dependent drifts, CO poisoning, low abundance and high cost [3,7-10]. These aspects hinder the commercialization of Pt for PEM (proton exchange membrane) fuel cells [11,12].

Recently, different forms of carbon materials are being explored for developing inexpensive and efficient electrocatalysts due to their high surface area, tunable pore size and large pore volume, which facilitates transportation of reactants and products [13,14]. Graphene and its derivatives, ordered mesoporous carbon, multi-walled carbon nanotubes etc. to name a few are widely being explored [10,15-20]. Graphene and its derivatives have received significant attention due to its excellent electronic, mechanical and thermal properties, and tunable band gap [21-23]. Doping with hetero-atoms has been reported to enhance the catalytic activity of materials as reported by Lindbergh *et al.*[24] and Mukerjee *et al.*[25] among others [26-28]. N-doped graphene has been reported to be comparable to Pt for ORR [11,25,29]. In particular, pyridinic and pyrrolic N are theorized to improve ORR by modifying band structure and density of states [11]. N doping can induce charge delocalization due to its high electronegativity, difference in bond length and atomic size resulting in $O_2$ molecule adsorption on two adjacent C atoms by side-on adsorption mode [15,30]. This results in weakening of O-O bond and reduction of $O_2$ to $H_2O$ [31]. P is similar to N in having the same number of electrons and hence is expected to behave similar chemically [32]. But due to its large atomic radius and high electron donating properties than N, it is believed to improve the catalytic properties to a greater extent [32]. Si due to its larger atomic radius and high electron donating ability is also expected to improve ORR.

Hetero-atom doped carbon materials are being produced by different techniques. Qu *et al.*[10] reported the synthesis of N-graphene by chemical vapor deposition (CVD) of $CH_4$ in presence of $NH_3$. Li *et al.*[33] reported N-graphene production by thermal annealing of graphene oxide in $NH_3$. Li *et al.*[34] and Panchakarla *et al.*[35] reported production of N-graphene by direct current arc-discharge of graphite electrodes with $NH_3$ and pyridine vapor respectively. Shao *et al.*[36] reported N-graphene synthesis from $N_2$ plasma treatment of graphene produced from thermal expansion of graphite oxides. Liu *et al.*[37] reported the production of P-doped graphite layers by pyrolysis of toluene and triphenylphosphine and Wang *et al.*[38] have reported the synthesis of N-doped mesoporous carbon by calcination of herring sperm DNA. All the aforementioned techniques involve utilization of specialized equipment, reducing gases, and higher temperatures for prolonged periods of time [36,39-45]. In this paper, N, P and Si tri-doped C (NPSiDC) materials synthesized by a rapid, one-pot microwave assisted method for ORR are reported. The reported technique is simple (no specialized equipment is needed, requires only a household commercial microwave oven), rapid (only 30 min synthesis duration), does not involve any inert/reducing gases and is high yielding [46]. Rao *et al.*[47] have reported that temperatures around 1550 K were attained with amorphous carbon in just 1 min of operation of a domestic microwave oven at 1.25 kW power. Further details about the microwave-assisted technique has been reported elsewhere [46].

Nitrogen doped carbon materials have been developed from different precursors including ethylenediamine [32,48,49], diaminopropane [49], cyanamide [50], pyridine [35], polymer precursors like polyphenylacetylene [51], poly(N-methyl pyrrole) [52] etc. which are toxic to humans [44]. This paper reports NPSiDCs prepared by utilization of a renewable resource material, thiamine, as a C and N source, Silicone fluid (500 cst) as Si source and ammonium polyphosphate as the microwave absorber and P and N source. The mixture of precursor materials on exposure to microwave radiation get rapidly heated to higher temperatures during which they decompose and react, liberating reducing gases which further assist in the carbonization and deoxygenation/reduction process. The NPSiDCs were extensively characterized by different techniques to understand the physio-chemical properties, which have been previously reported [53]. These NPSiDCs were investigated as electrocatalysts to facilitate ORR under alkaline conditions, which is discussed in this paper.

## 2. MATERIALS AND METHODS

### *2.1. Materials*

The details regarding chemicals including Thiamine hydrochloride, Silicon fluid 500 cst and Ammonium polyphosphate was reported previously [53]. Potassium hydroxide was purchased from Fischer Chemicals, New Jersey.

### *2.2. Synthesis of N, P and Si tri-doped C from thiamine hydrochloride*

Synthesis of NPSiDCs was performed using a novel microwave-assisted method without employing any inert/reducing gases. Pre-determined amounts of silicone fluid and ammonium polyphosphate were weighed into a boron nitride crucible and mixed thoroughly using a glass rod. To this mixture, pre-weighed amount of thiamine hydrochloride was added and mixed well using a glass rod. This mixture was heated for 30 min using a similar cap and an $Al_2O_3$ cover in an $Al_2O_3$ muffle with an $Al_2O_3$ lid using a commercial table-top microwave oven operating at 2.45 GHz and 1.25 kW power. After the microwave heating duration, the product was allowed to cool, weighed and ground well. The details of synthesis procedure of NPSiDCs have been reported previously [53]. The chemical structure of thiamine can be seen in Figure 1.

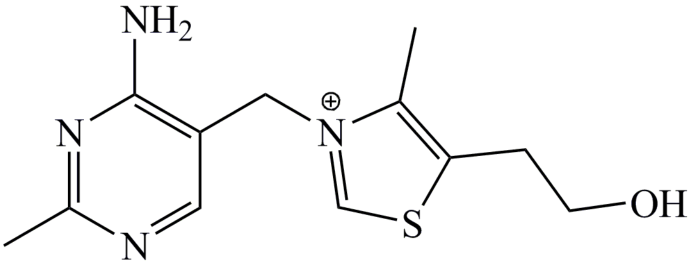

**Figure 1.** The chemical structure of thiamine.

### *2.3. Electrochemical studies*

All electrochemical measurements were carried out using AFCBP1 bipotentiostat from Pine Instrument Company using a three electrode system comprising of glassy carbon (5 mm diameter and 0.196 $cm^2$ geometric area in polytetrafluoroethylene holder) working electrode, Hg/HgO reference electrode and a Pt wire counter electrode. However, all the results were reported with reference to RHE (Reversible Hydrogen Electrode) so as to enable comparsion with similar studies reported earlier. A 0.1M KOH aqueous solution was used as the electrolyte. The electrolyte was purged with $O_2$ for 30 min before the measurements were recorded and an $O_2$ blanket above the solution was maintained during the studies. During control experiments, the electrolyte was saturated with $N_2$ to minimize the interference from $O_2$. The glassy carbon electrode was cleaned by polishing the electrode surface using a 0.5 μ alumina paste followed by rinsing with distilled water. A 1 mg/mL suspension of electrode material in ethanol was prepared by sonication for 1 h. To 0.5 mL of this suspension, 20 uL Nafion was added and sonicated for an additional 10 min. A 10 uL aliquot of this suspension was drop-casted onto glassy carbon electrode, air dried, followed by addition of another 10 uL aliquot, air dried and finally dried well in vacuum for 10 min. The modified glassy carbon electrode was utilized for electrochemical measurements.

## 3. RESULTS AND DISCUSSION

### *3.1. Characterization results*

All the physicochemical characterization results of NPSiDCs discussed here were reported earlier [53]. However, a brief overview is presented here solely for better understanding.

Scanning electron microscopic (SEM) analysis revealed NPSiDCs to have several irregular structures [53]. SEM images have been reported previously [53].

$N_2$ adsorption desorption studies were performed on powder samples of NPSiDCs. The isotherms were classified as type IV according to IUPAC with H4 hysteresis loop indicating the presence of slit shaped pores [53]. The Brunauer-Emmett-Teller (BET) specific surface area of NPSiDC-1, NPSiDC-2 and NPSiDC-3 was found out to be 471.04 $m^2$ $g^{-1}$, 228.34 $m^2$ $g^{-1}$ and 231.38 $m^2$ $g^{-1}$ respectively. The pore size distribution curves indicate that majority of pores are distributed in the mesoporous size range. Single point total pore volume of NPSiDC-1, NPSIDC-2 and NPSiDC-3 was found out to be 0.25, 0.15 and 0.17 $cm^3$ $g^{-1}$ respectively [53]. The development of diverse pores in NPSiDCs can be attributed to the microwave assisted method employed for synthesizing NPSiDCs during which reducing gases were liberated which help in creating pores. $N_2$ adsorption desorption isotherms and pore size distribution curves have been reported previously [53].

Surface elemental analysis from X-ray Photoelectron Spectroscopy (XPS) revealed NPSiDCs to be composed mainly of C, O and Si with little amounts of N and P. NPSiDC-1 was found to contain 56. 8% C, 28.7% O, 10.0% Si, 2.2% N and 2.3% P; NPSiDC-2 was found to contain 30.5% C, 46.7% O, 17.3% Si, 1.9% N and 3.7% P while NPSiDC-3 contains 27.1% C, 54.2% O, 17.3% Si, 0.6% N and 0.9% P. Even though thiamine hydrochloride contains S, no measurable amount of S was observed in NPSiDCs. XPS narrow scan analysis of NPSiDCs has been reported previously [53].

### *3.2. Results from electrochemical studies*

The cyclic voltammograms of NPSiDC-1, NPSiDC-2 and NPSiDC-3 recorded in 0.1M KOH are shown in Figure 2, Figure 3 and Figure 4 respectively. A clear sharp reduction peak at 0.548 V, 0.542 V and 0.575 V vs. RHE was observed with NPSiDC-1, NPSiDC-2 and NPSiDC-3 respectively.

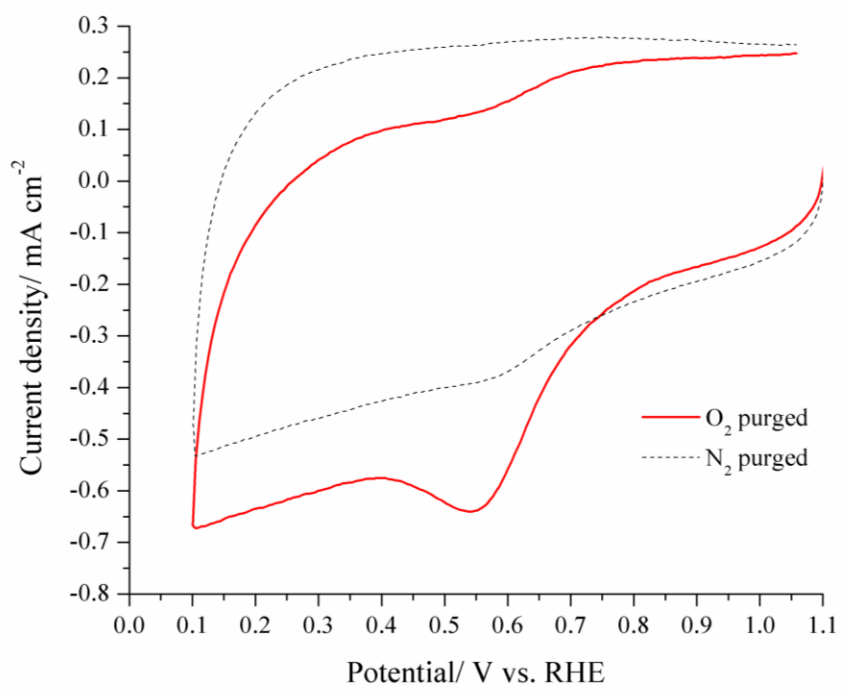

**Figure 2.** Cyclic voltammograms of NPSiDC-1 recorded in $N_2$ saturated and $O_2$ saturated 0.1M KOH at a scan rate of 100 mV s$^{-1}$.

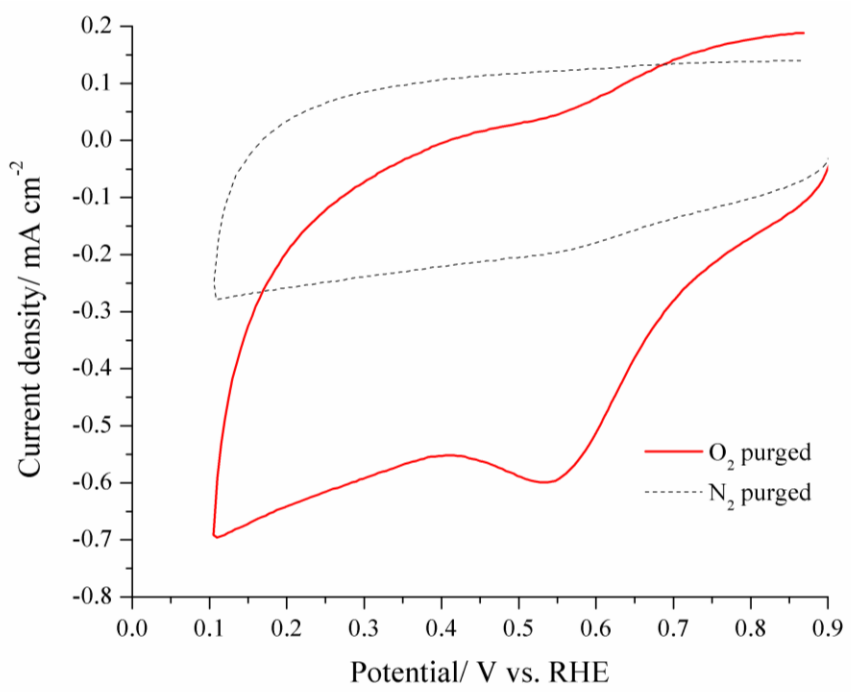

**Figure 3.** Cyclic voltammograms of NPSiDC-2 recorded in $N_2$ saturated and $O_2$ saturated 0.1M KOH at a scan rate of 100 mV s$^{-1}$.

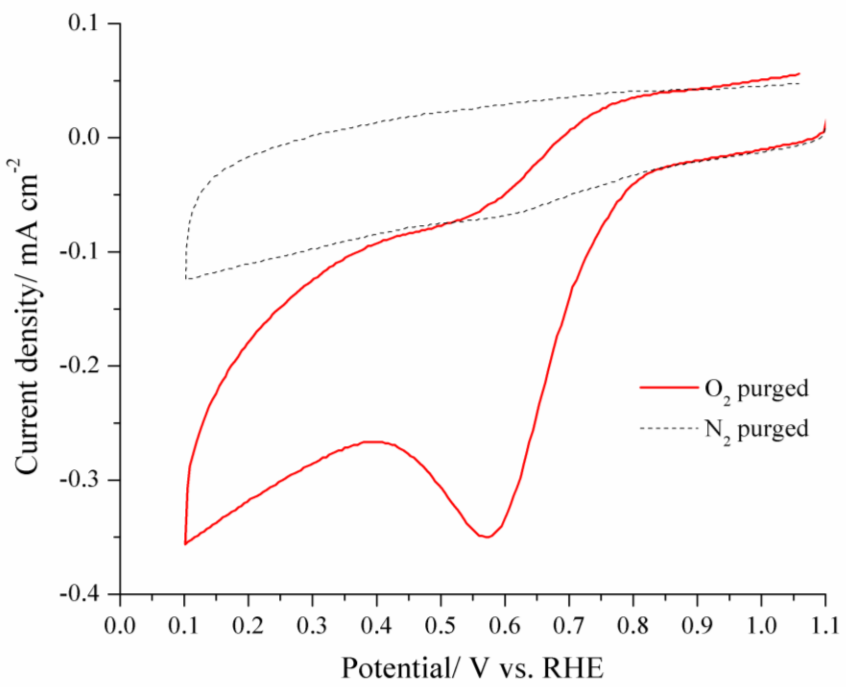

**Figure 4.** Cyclic voltammograms of NPSiDC-3 recorded in $N_2$ saturated and $O_2$ saturated 0.1M KOH at a scan rate of 100 mV s$^{-1}$.

**Table 1.** Summary of onset peak potential and $O_2$ reduction peak potential values of NPSiDC samples.

| Sample | Onset potential (V) | Peak potential (V) |
|---|---|---|
| **NPSiDC-1** | 0.722 | 0.548 |
| **NPSiDC-2** | 0.703 | 0.542 |
| **NPSiDC-3** | 0.755 | 0.575 |

The $O_2$ reduction peak due to NPSiDC-3 was observed to be very prominent and towards more positive potential value compared to other NPSiDCs. To confirm that the peak is due to reduction of $O_2$, a control was performed in the absence of $O_2$ by saturating the electrolyte with $N_2$. No clear reduction peak was observed under $O_2$-free conditions confirming that the peak observed under $O_2$ saturated conditions was due to $O_2$ reduction, which indicates the potential of NPSiDCs for ORR. NPSiDC-1, NPSiDC-2 and NPSiDC-3 exhibit onset potential at 0.722 V, 0.703 V and 0.755 V respectively. The peak onset potential value with NPSiDC-3 is also towards more positive potential value compared to other NPSiDC samples. Also, as seen from the Figures 2, 3 and 4, NPSiDCs exhibit good current density. The onset potential and $O_2$ reduction peak potential values of NPSiDCs are reported in Table 1. The ORR performance of NPSiDCs was found to be comparable to other non-metal based electrocatalysts reported previously [9,29,44,48,54,55].

The linear sweep voltammograms were recorded at different rotation speeds of 100 rpm, 400 rpm, 900 rpm, 1600 rpm and 2500 rpm at a scan rate of 10 mV $s^{-1}$ in $O_2$ saturated 0.1M KOH to elucidate the mechanism of $O_2$ reduction by NPSiDCs. From Koutecky-Levich plots, the number of $e^-$ involved in the ORR can be calculated based on the following equations [10,29].

$$1/j_{lim} = 1/j_{Lev} + 1/j_k$$

$$j_{Lev} = 0.620nFCD^{2/3}\omega^{1/2}\upsilon^{-1/6}$$

where, $j_{lim}$, $j_{Lev}$ and $j_k$ are the measured current density, Levich (or diffusion) current density and the kinetic current density respectively, n is the number of $e^-$ involved in the transfer process, F is the Faraday constant (F = 96485 C $mol^{-1}$), C is the bulk concentration of $O_2$ (C = 2.4 x $10^{-4}$ M at 22 °C), D is the diffusion coefficient of $O_2$ in water at 22 °C (D = 1.7 x $10^{-5}$ $cm^2$ $s^{-1}$), $\upsilon$ is the kinematic viscosity of the electrolyte at 22 °C ($\upsilon$ = 0.01 $cm^2$ $s^{-1}$) and $\omega$ (= $2\pi N$, where N is the linear rotation speed) is the angular velocity of the electrode.

Figure 5, Figure 6 and Figure 7 demonstrate the rotating disk electrode (RDE) voltammograms of NPSiDCs recorded at different rotation speeds at a scan rate of 10 mV $s^{-1}$. The limiting current density values were measured from each voltammogram. A reciprocal of limiting current density versus reciprocal square root of angular rotation speed from each linear sweep voltammogram yields K-L plot. The experimental results were compared with theoretical 2 $e^-$ and 4 $e^-$ processes for each NPSiDC which can be seen in Figures 8 - 10. The number of $e^-$ involved in the ORR can be computed from the slope of the straight line ($1/(0.620nFCD^{2/3}\upsilon^{-1/6})$). The experimentally determined n value was found to be close to the theoretically proposed value of 4. Table 2 reports the n value of NPSiDCs determined from RDE voltammograms and K-L plot.

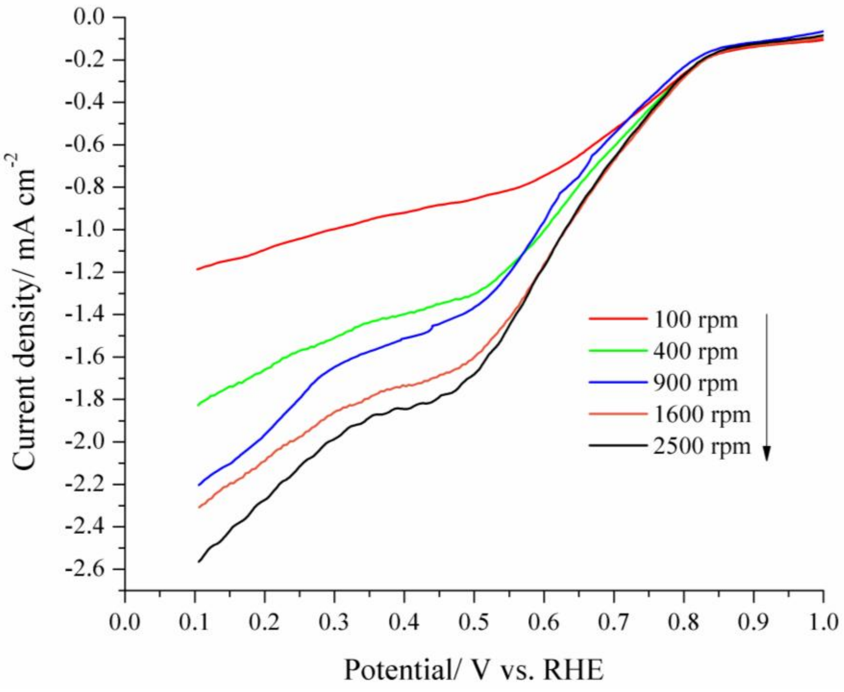

**Figure 5.** RDE curves of NPSiDC-1 recorded at different rotation speeds in $O_2$ saturated 0.1M KOH.

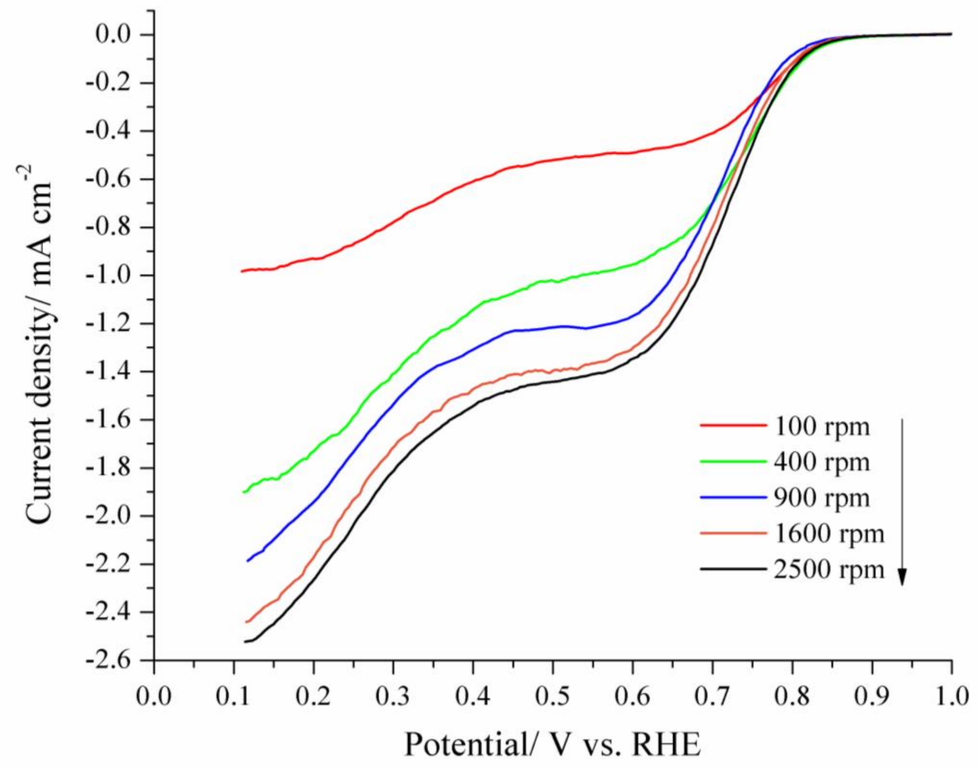

**Figure 6.** RDE curves of NPSiDC-2 recorded at different rotation speeds in $O_2$ saturated 0.1M KOH.

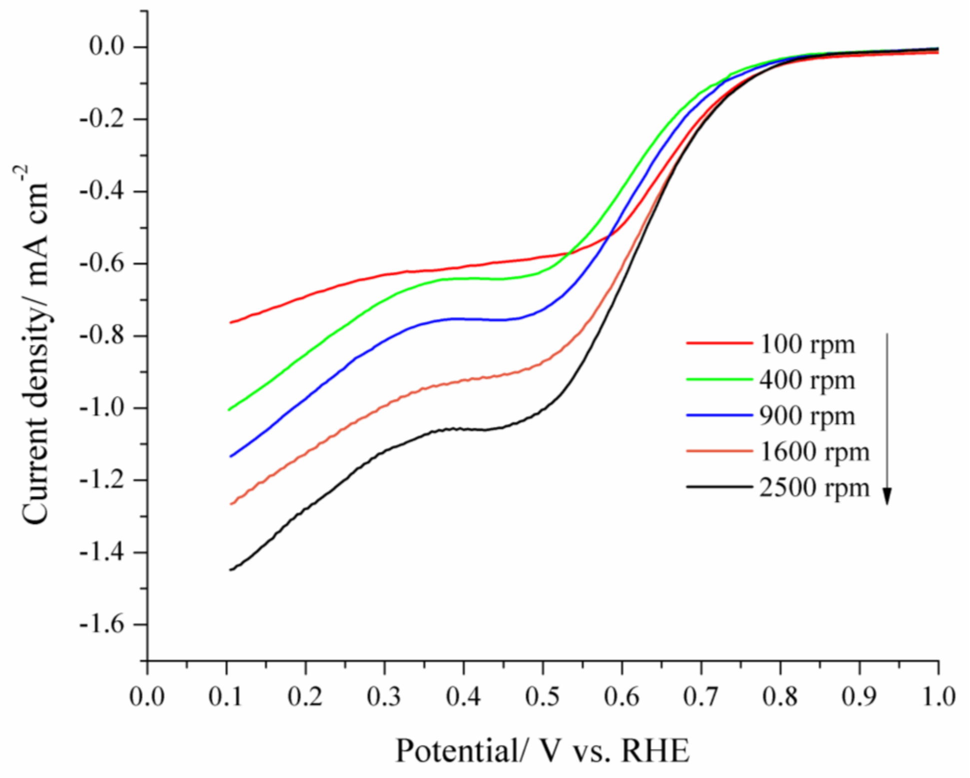

**Figure 7.** RDE curves of NPSiDC-3 recorded at different rotation speeds in $O_2$ saturated 0.1M KOH.

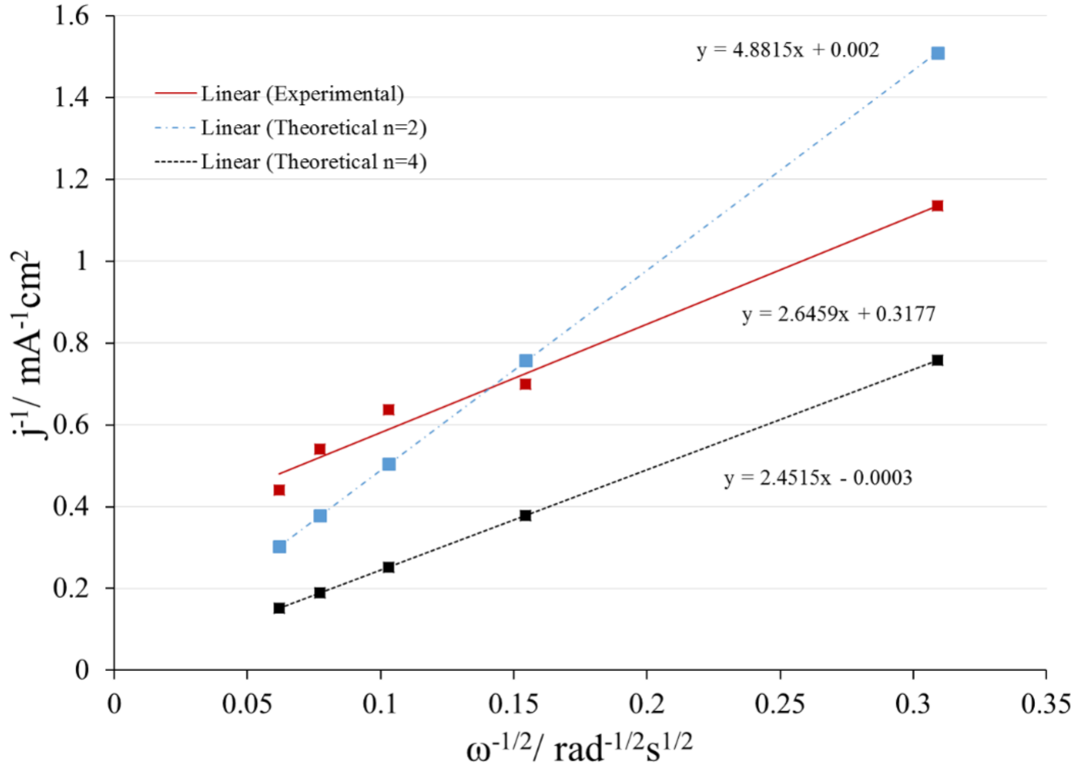

**Figure 8.** K-L plots of NPSiDC-1, theoretical 2 $e^-$ and 4 $e^-$ $O_2$ reduction processes**.**

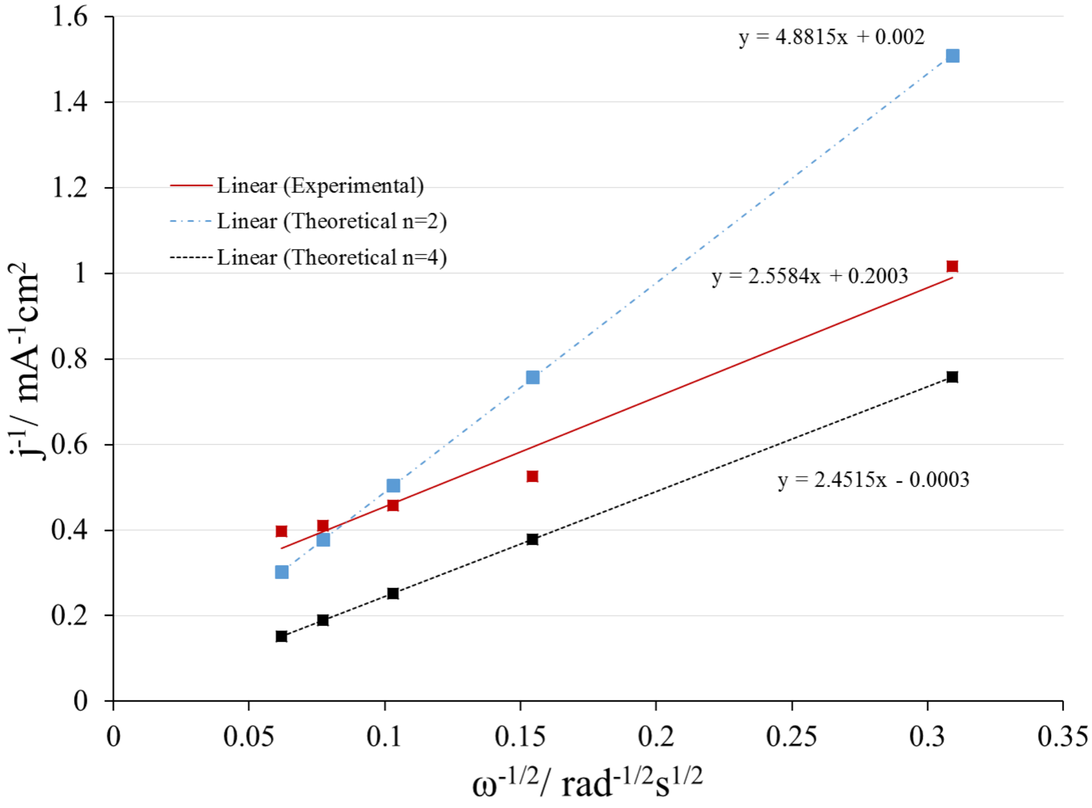

**Figure 9.** K-L plots of NPSiDC-2, theoretical 2 $e^-$ and 4 $e^-$ $O_2$ reduction processes.

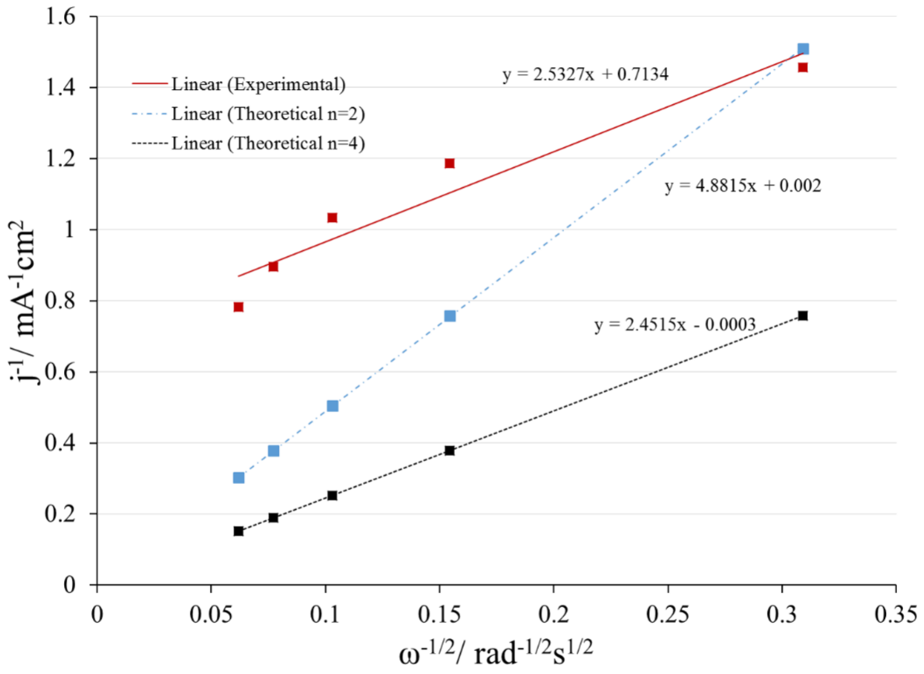

**Figure 10.** K-L plots of NPSiDC-3, theoretical 2 $e^-$ and 4 $e^-$ $O_2$ reduction processes.

**Table 2.** Number of $e^-$ involved in ORR of NPSiDCs calculated from RDE results.

| Sample | n value (based on RDE results) |
|---|---|
| **NPSiDC-1** | 3.70 |
| **NPSiDC-2** | 3.83 |
| **NPSiDC-3** | 3.87 |

RRDE studies were performed at a rotation speed of 1600 rpm and scan rate of 50 mV $s^{-1}$ in $O_2$ saturated 0.1M KOH. Figure 11, Figure 12 and Figure 13 demonstrate the RRDE plots of NPSiDCs. As observed from Figures 11 - 13, the ring current density is negligible compared to the disk current density, thus indicating only a very little generation of $HO_2^-$ species and hence the $O_2$ reduction capability of NPSiDCs. Also, using ring current and disk current values from RRDE plots the number of $e^-$ involved in the ORR can be computed using the following equation [56].

$$n = 4I_{disk} / (I_{disk} + (I_{ring} / N))$$

where, n is the number of electrons involved in the transfer process, $I_{disk}$ is the disk current, $I_{ring}$ is the ring current and N is the collection efficiency of the electrode (0.256).

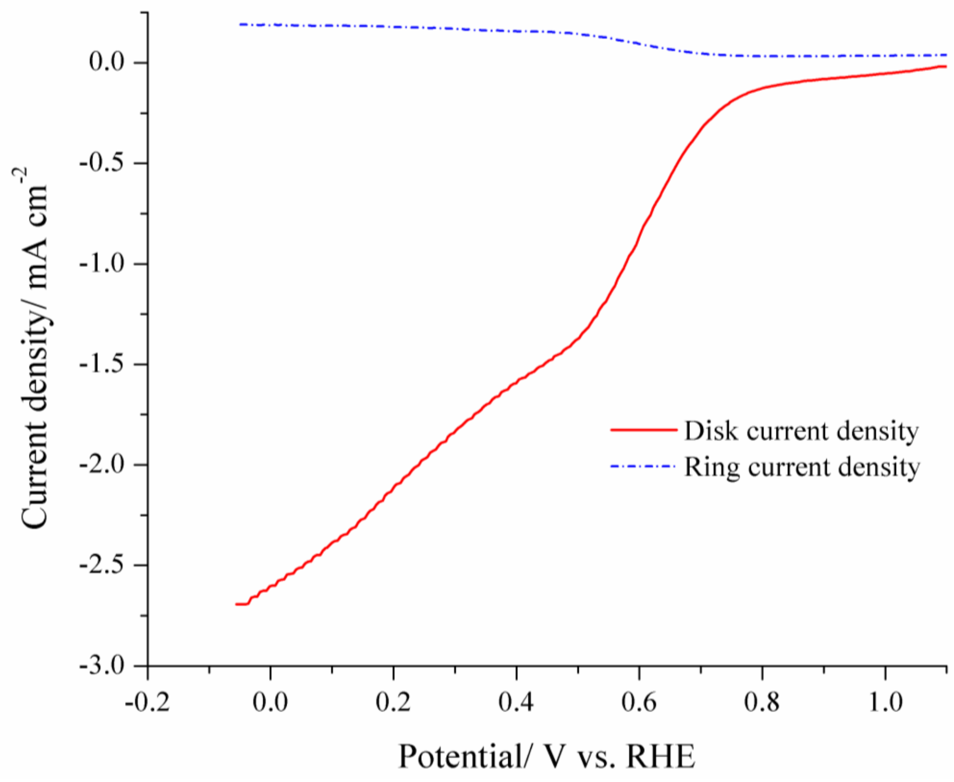

**Figure 11.** RRDE plot of NPSiDC-1 in $O_2$ saturated 0.1M KOH at rotation speed of 1600 rpm.

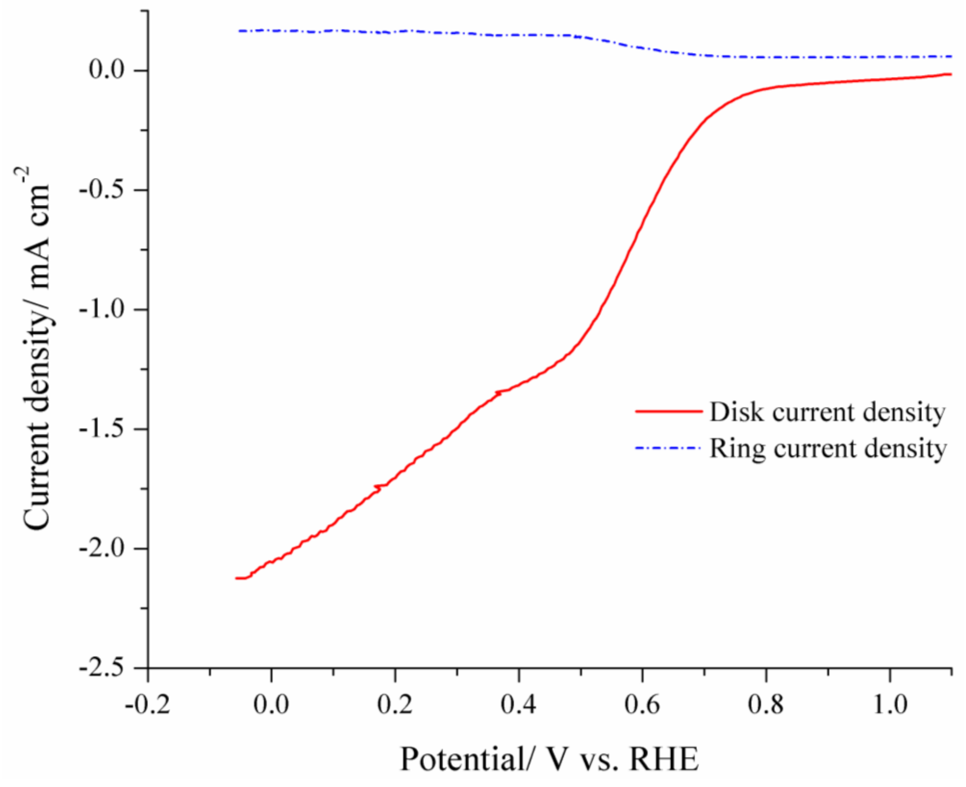

**Figure 12.** RRDE plot of NPSiDC-2 in $O_2$ saturated 0.1M KOH at rotation speed of 1600 rpm.

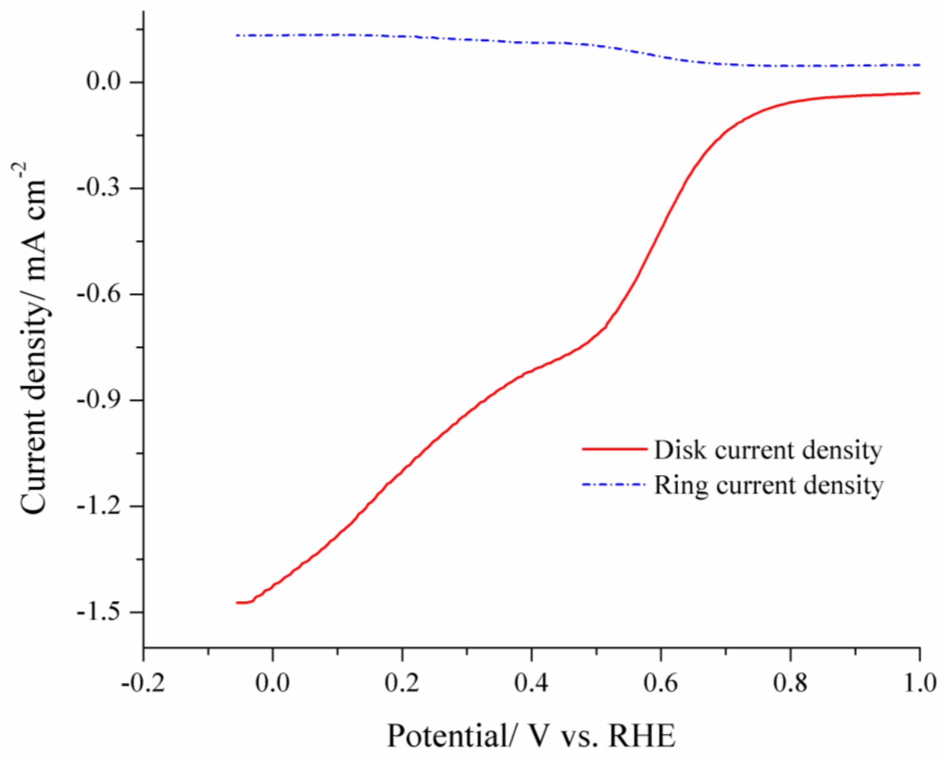

**Figure 13.** RRDE plot of NPSiDC-3 in $O_2$ saturated 0.1M KOH at rotation speed of 1600 rpm.

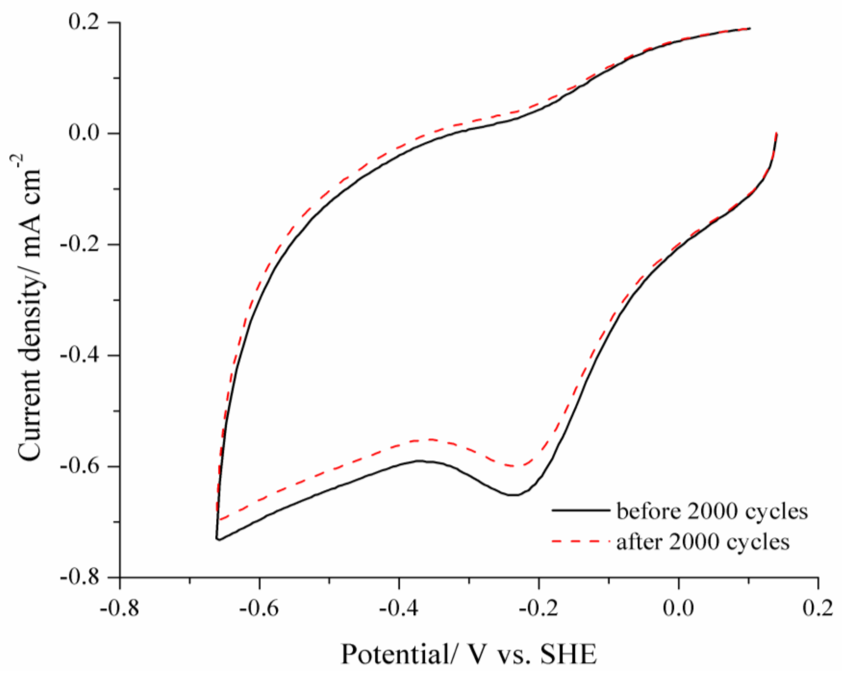

**Figure 14.** Cyclic voltammograms of NPSiDC-2 recorded in $O_2$ saturated 0.1M KOH before and after 2000 cycles at 100 mV s$^{-1}$.

Based on the RDE (and as indicated by RRDE) results the mechanism of $O_2$ reduction by NPSiDCs can be confirmed to be a 4e$^-$ mediated process and the following mechanism is proposed:

$O_2 + 2\,H_2O + 4\,e^- \rightarrow 4\,OH^-$

A combination of factors including surface area, porosity and dopants can be attributed to the optimum ORR performance of NPSiDCs. High surface area and porosity allows analyte moieties ($O_2$) to easily access the active centers in the electrocatalyst whereas dopants like N by virtue of its electronegativity render adjacent C atoms as active centers for ORR [15,30]. Other dopants like Si and P due to their low electronegativity than adjacent C themselves may catalyze the ORR [8,54,57].

To investigate the electrochemical stability of NPSiDCs, stability studies were performed with a typical NPSiDC sample. The cyclic voltammograms of NPSiDC-2 recorded before and after the generation of continuous 2000 cycles in $O_2$ saturated 0.1M KOH at 100 mV $s^{-1}$ can be seen in Figure 14. It is observed that there is no significant decrease in ORR activity of NPSiDC-2 even after 2000 cycles.

## 4. SUMMARY OF THE WORK

NPSiDCs developed from thiamine as renewable resource material exhibit promise for ORR under alkaline conditions. NPSiDC-1, NPSiDC-2 and NPSiDC-3 exhibit $O_2$ reduction peak potential values at 0.548 V, 0.542 V and 0.575 V respectively vs. RHE in 0.1M KOH. From RDE studies and K-L plot, the mechanism of ORR was investigated. The number of $e^-$ for all the three electrocatalysts was observed to be close to 4, indicating their capability towards ORR. This observation was further confirmed by almost zero ring current density from RRDE studies. No drastic decrease in ORR performance with NPSiDC-2 was observed over 2000 cycles indicating its electrochemical stability.

ACKNOWLEDGEMENTS
The authors would like to acknowledge the Centre for Integrative Nanotechnology Sciences, University of Arkansas at Little Rock for the equipment utilized in characterization of materials. The authors would also like to acknowledge the partial financial support received through NASA Research Infrastructure Development grant.

## References

1. B. Wang, *J. Power Sources*, 152 (2005) 1
2. Y. Wang and P. B. Balbuena, *J. Phys. Chem. B*, 109 (2005) 14896
3. R. Holze, *Recent trends in fuel cell science and technology: Edited by S. Basu*, 2009
4. G. Che, B. B. Lakshmi, E. R. Fisher and C. R. Martin, *Nature*, 393 (1998) 346
5. K. Gong, P. Yu, L. Su, S. Xiong and L. Mao, *J. Phys. Chem. C*, 111 (2007) 1882
6. A. Kongkanand, S. Kuwabata, G. Girishkumar and P. Kamat, *Langmuir*, 22 (2006) 2392
7. M. Winter and J. Brodd Ralph, *Chem Rev*, 104 (2004) 4245
8. M. Zhang and L. Dai, *Nano Energy*, 1 (2012) 514
9. Z. Yang, H. Nie, X.-a. Chen, X. Chen and S. Huang, *J. Power Sources*, 236 (2013) 238
10. L. Qu, Y. Liu, J.-B. Baek and L. Dai, *ACS Nano*, 4 (2010) 1321
11. L. Zhang, J. Niu, L. Dai and Z. Xia, *Langmuir*, 28 (2012) 7542
12. D.-S. Yang, D. Bhattacharjya, S. Inamdar, J. Park and J.-S. Yu, *J. Am. Chem. Soc.*, 134 (2012) 16127

13. S. B. Yoon, G. S. Chai, S. K. Kang, J.-S. Yu, K. P. Gierszal and M. Jaroniec, *J. Am. Chem. Soc.*, 127 (2005) 4188
14. T.-W. Kim, H.-D. Kim, K.-E. Jeong, H.-J. Chae, S.-Y. Jeong, C.-H. Lee and C.-U. Kim, *Green Chem.*, 13 (2011) 1718
15. K. Gong, F. Du, Z. Xia, M. Durstock and L. Dai, *Science*, 323 (2009) 760
16. W. Xiong, F. Du, Y. Liu, A. Perez, M. Supp, T. S. Ramakrishnan, L. Dai and L. Jiang, *J. Am. Chem. Soc.*, 132 (2010) 15839
17. T. C. Nagaiah, S. Kundu, M. Bron, M. Muhler and W. Schuhmann, *Electrochem. Commun.*, 12 (2010) 338
18. Y. Tang, B. L. Allen, D. R. Kauffman and A. Star, *J. Am. Chem. Soc.*, 131 (2009) 13200
19. R. Liu, D. Wu, X. Feng and K. Muellen, *Angewandte Chemie*, 49 (2010) 2565
20. W. Yang, T.-P. Fellinger and M. Antonietti, *J. Am. Chem. Soc.*, 133 (2011) 206
21. K. I. Bolotin, K. J. Sikes, Z. Jiang, M. Klima, G. Fudenberg, J. Hone, P. Kim and H. L. Stormer, *Solid State Commun.*, 146 (2008) 351
22. A. A. Balandin, S. Ghosh, W. Bao, I. Calizo, D. Teweldebrhan, F. Miao and C. N. Lau, *Nano Lett.*, 8 (2008) 902
23. R. R. Nair, P. Blake, A. N. Grigorenko, K. S. Novoselov, T. J. Booth, T. Stauber, N. M. R. Peres and A. K. Geim, *Science (Washington, DC, U. S.)*, 320 (2008) 1308
24. F. Jaouen, S. Marcotte, J.-P. Dodelet and G. Lindbergh, *J. Phys. Chem. B*, 107 (2003) 1376
25. K. Strickland, E. Miner, Q. Jia, U. Tylus, N. Ramaswamy, W. Liang, M.-T. Sougrati, F. Jaouen and S. Mukerjee, *Nat. Commun.*, 6 (2015) 7343
26. Y. Zheng, Y. Jiao, M. Jaroniec, Y. Jin and S. Z. Qiao, *Small*, 8 (2012) 3550
27. H. Jin, H. Zhang, H. Zhong and J. Zhang, *Energy Environ. Sci.*, 4 (2011) 3389
28. C. P. Ewels and M. Glerup, *J. Nanosci. Nanotechnol.*, 5 (2005) 1345
29. Y. Sun, C. Li and G. Shi, *J. Mater. Chem.*, 22 (2012) 12810
30. K. N. Kudin, B. Ozbas, H. C. Schniepp, R. K. Prud'homme, I. A. Aksay and R. Car, *Nano Lett.*, 8 (2008) 36
31. Y. Shao, J. Liu, Y. Wang and Y. Lin, *J. Mater. Chem.*, 19 (2009) 46
32. S. Yang, X. Feng, X. Wang and K. Muellen, *Angewandte Chemie*, 50 (2011) 5339
33. Y. Li, Z. Huang, K. Huang, D. Carnahan and Y. Xing, *Energy Environ. Sci.*, 6 (2013) 3339
34. N. Li, Z. Wang, K. Zhao, Z. Shi, Z. Gu and S. Xu, *Carbon*, 48 (2009) 255
35. L. S. Panchakarla, K. S. Subrahmanyam, S. K. Saha, A. Govindaraj, H. R. Krishnamurthy, U. V. Waghmare and C. N. R. Rao, *Adv. Mater.*, 21 (2009) 4726
36. Y. Shao, S. Zhang, M. H. Engelhard, G. Li, G. Shao, Y. Wang, J. Liu, I. A. Aksay and Y. Lin, *J. Mater. Chem.*, 20 (2010) 7491
37. Z.-W. Liu, F. Peng, H.-J. Wang, H. Yu, W.-X. Zheng and J. Yang, *Angew. Chem., Int. Ed.*, 50 (2011) 3257
38. X. Wang, X. Li, L. Zhang, Y. Yoon, P. K. Weber, H. Wang, J. Guo and H. Dai, *Science*, 324 (2009) 768
39. D. Geng, Y. Chen, Y. Chen, Y. Li, R. Li, X. Sun, S. Ye and S. Knights, *Energy Environ. Sci.*, 4 (2011) 760
40. Z. Wen, S. Ci, F. Zhang, X. Feng, S. Cui, S. Mao, S. Luo, Z. He and J. Chen, *Adv. Mater.*, 24 (2012) 1399
41. Y. Wang, Y. Shao, D. W. Matson, J. Li and Y. Lin, *ACS Nano*, 4 (2010) 1790
42. D. Chen, L. Tang and J. Li, *Chem. Soc. Rev.*, 39 (2010) 3157
43. S. Wang, L. Zhang, Z. Xia, A. Roy, D. W. Chang, J.-B. Baek and L. Dai, *Angew. Chem., Int. Ed.*, 51 (2012) 4209
44. H. Wang, X. Bo, C. Luhana and L. Guo, *Electrochem. Commun.*, 21 (2012) 5
45. Z. Lin, G. Waller, Y. Liu, M. Liu and C.-P. Wong, *Adv. Energy Mater.*, 2 (2012) 884
46. T. Viswanathan, US 2013/0157838 A1 (2011).

47. K. J. Rao, B. Vaidhyanathan, M. Ganguli and P. A. Ramakrishnan, *Chem. Mater.*, 11 (1999) 882
48. X. Zhou, Z. Yang, H. Nie, Z. Yao, L. Zhang and S. Huang, *J. Power Sources*, 196 (2011) 9970
49. D. Higgins, Z. Chen and Z. Chen, *Electrochim. Acta*, 56 (2010) 1570
50. K. Kwon, Y. J. Sa, J. Y. Cheon and S. H. Joo, *Langmuir*, 28 (2012) 991
51. W. Z. Yuan, J. Z. Sun, Y. Dong, M. Haeussler, F. Yang, H. P. Xu, A. Qin, J. W. Y. Lam, Q. Zheng and B. Z. Tang, *Macromolecules*, 39 (2006) 8011
52. B. Narsimha Reddy, N. Billa and M. Deepa, *ChemPlusChem*, 77 (2012) 789
53. S. K. Ramasahayam, Z. Hicks and T. Viswanathan, *ACS Sustainable Chem. Eng.*, 3 (2015) 2194
54. D. Yu, Y. Xue and L. Dai, *J. Phys. Chem. Lett.*, 3 (2012) 2863
55. Z. Mo, S. Liao, Y. Zheng and Z. Fu, *Carbon*, 50 (2012) 2620
56. M. Chisaka, T. Iijima, Y. Ishihara, Y. Suzuki, R. Inada and Y. Sakurai, *Electrochim. Acta*, 85 (2012) 399
57. C. H. Choi, S. H. Park and S. I. Woo, *ACS Nano*, 6 (2012) 7084